

M agnetic properties of a  $S = 1/2$  zigzag spin chain com pound  $(N_2H_5)CuCl_3$

N . M aeshim a,<sup>1</sup> M . H agiwara,<sup>2</sup> Y . N arum i,<sup>3</sup> K . K indo,<sup>4</sup> T . C . K obayashi,<sup>4</sup> and K . O kunish<sup>5</sup>

<sup>1</sup> D epartm ent of Engineering, O saka E lectro-C om m unication University, Neyagawa, O saka 572-8530, Japan

<sup>2</sup> R IKEN (The Institute of Physical and Chemical Research), W ako, Saitam a 351-0198, Japan

<sup>3</sup> R IKEN Harim a Institute, Sayo, Hyogo 679-5148, Japan

<sup>4</sup> K YOKUGEN, O saka University, Toyonaka, O saka 560-8531, Japan

<sup>5</sup> D epartm ent of Physics, Faculty of Science, Niigata University, Niigata 950-2181, Japan

(D ated: M ay 21, 2019)

W e present a theoretical and experim ental study of a quasi-one-dim ensional zigzag antiferrom agnet  $(N_2H_5)CuCl_3$ , which can be viewed as weakly coupled Heisenberg chains with a frustrated interaction. W e first discuss generic features of the m agnetic properties of the zigzag spin chains between the nearly single chain case and the nearly double chain case, on the basis of the finite temperature density-m atrix renom alization group (DM RG) calculations. W e next show the experim ental results for the m agnetic susceptibility and the high- eld m agnetization of a single crystal of  $(N_2H_5)CuCl_3$  above the Neel temperature  $T_N = 1.55K$ . By com paring the experim ental data with the DM RG results carefully, we finally determ ine the ratio of the nearest and next-nearest exchange couplings as  $J_1=J_2 = 0.25$  with  $J_2/k_B = 16.3K$ .

PACS num bers: 05.10.Lc, 75.10.Jm, 75.40.Cx, 75.50.Ee

I. INTRODUCTION

Frustration e ects in low -dim ensional antiferrom agnetic (AF) quantum spin system s have attracted m uch attention because of their peculiar behavior in low -energy physics. The quantum e ect and the geom etrical frustration induce strong fluctuation cooperatively, which often gives rise to various non-m agnetic ground states and quantum phase transitions.<sup>1,2,3,4,5</sup>

A typical exam ple of such frustrated low -dim ensional m agnets is the  $S = 1/2$  antiferrom agnetic zigzag chain (see Fig. 1). The Hamiltonian of the zigzag spin chain is given by

$$H = \sum_i \left[ g_B H + \sum_i (J_1 S_i \cdot S_{i+1} + J_2 S_i \cdot S_{i+2}) \right] + \sum_i X S_i^z; \tag{1}$$

where  $S$  is the  $S = 1/2$  spin operator,  $g$  is the Land e's  $g$  factor and  $\mu_B$  is the Bohr m agneton.  $J_1$  and  $J_2$  denote the nearest neighbor and the next-nearest neighbor coupling constants respectively, and  $H$  is the applied m agnetic eld. Intensive theoretical studies have shown that the zigzag chain has a rich phase structure at the zero m agnetic eld. W hen  $J_2 = 0$ , the system is equivalent to the Heisenberg chain having the gapless excitation.<sup>6</sup> Increasing  $J_2$ , a quantum phase transition from the critical spin liquid phase to the gapped dimer phase<sup>2,7</sup> occurs at  $J_2=J_1 = 0.2411$ .<sup>8</sup> This gapped dimer phase is expected to extend up to the limit  $J_2=J_1 = 1$ ,<sup>9</sup> which corresponds to the two decoupled Heisenberg chains. Here, it should be rem arked that the dimer gap for  $J_1 \neq J_2$  is exponentially sm all:  $\exp(-\text{const}J_2=J_1)$ .<sup>9</sup>

The theoretical studies m entioned above have stim ulated experim ental studies of the zigzag spin chain. In fact, the m agnetic properties of  $SrCuO_2$ <sup>10</sup> and  $Cu[2-(2\text{-am inoethyl})pyridine]$ <sup>11</sup> were investigated recently.

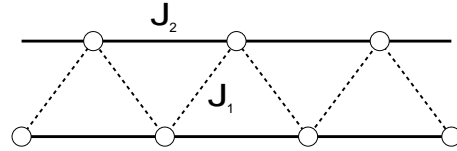
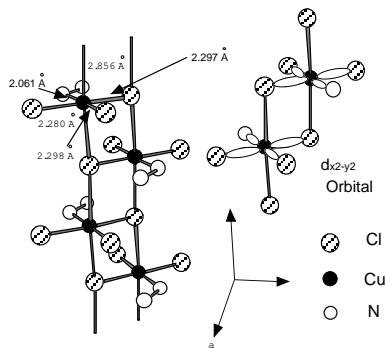


FIG. 1: The zigzag spin chain. The dashed lines and solid lines denote the nearest neighbor coupling  $J_1$  and the next-nearest neighbor coupling  $J_2$  respectively.

For the latter case, the nearly gapless behavior of the m agnetic susceptibility was observed for a powder sam ple, and then the ratio of the couplings of  $Cu[2-(2\text{-am inoethyl})pyridine]$  is estimated as  $J_2=J_1 = 0.2$ .<sup>11</sup> In this paper, we focus on another type of the zigzag com pound  $(N_2H_5)CuCl_3$ ,<sup>12</sup> which is interestingly expected to have the coupling constant  $J_1 \neq J_2$ .<sup>13</sup> Since  $(N_2H_5)CuCl_3$  can be synthesized as a single crystal, we can precisely com pare its m agnetic properties with num erical calculations.

An im portant point on the com pound is that its m agnetic property is very sim ilar to the one in the single Heisenberg chain limit, although it has the double chain structure. Thus how we can distinguish the m agnetic behavior of the zigzag chains between  $J_1 \neq J_2$  and  $J_1 = J_2$  is an im portant problem from both theoretical and experim ental views. In what follows, we study the m agnetic properties of a single crystal sam ple of  $(N_2H_5)CuCl_3$ , on the basis of the precise com parison between the results of accurate num erical calculations and the experim ental m easurem ents of the m agnetic susceptibility and the high- eld m agnetization.

In Sec. II, we describe the fundam ental aspects of the single crystal of  $(N_2H_5)CuCl_3$  and the finite temperature density m atrix renom alization group (DM RG) method.<sup>14,15</sup> In Sec. III, we show the DM RG results for

FIG. 2: Chain structure of  $(\text{N}_2\text{H}_5)\text{CuCl}_3$ .

the susceptibility and the magnetization curve, and discuss generic features of them. In Sec. IV we show the experimental data of the magnetic susceptibility and the high-field magnetization parallel to the chain direction. Then the exchange coupling  $J_2 = k_B = 16.3$  K and the ratio  $J_1 = J_2 = 0.25$  are determined by the precise comparison of the experimental data with the DM RG results. In Sec. V the conclusion is summarized.

## II. EXPERIMENTAL AND COMPUTATIONAL DETAILS

### A. experiment

First we summarize the synthesis and the crystal structure of  $(\text{N}_2\text{H}_5)\text{CuCl}_3$ . Single crystal samples of  $(\text{N}_2\text{H}_5)\text{CuCl}_3$  were synthesized by the method described in Ref. 12. Chemical analysis shows good agreement between the observed and calculated ratios of the elements. This compound crystallizes in the orthorhombic system (space group:  $Pnm2_1$ ).<sup>12</sup> The lattice constants at room temperature are  $a = 14.439(2)$  Å,  $b = 5.705(1)$  Å, and  $c = 6.859(1)$  Å. The chain structure of this compound is shown in Fig. 2. This compound has the ladder structure in which Cu and Cl align alternately along the leg, forming a copper zigzag chain. Copper 3d hole orbitals ( $3d_{x^2-y^2}$ ) are situated perpendicularly to the leg, resulting in small exchange interactions along the leg.

Magnetic susceptibilities were measured with a SQUID magnetometer (Quantum Design's MPMS-XL7) installed at KYOKUGEN in Osaka University. High-field magnetization measurements up to 30T were carried out with a pulse magnet at the same place. Besides, X-band ESR (Varian E109 spectrometer) and specific heat measurements were carried out at the same place.

In order to obtain reliable numerical data, we employ the finite temperature DM RG method.<sup>14,15</sup> Since this method is free from the negative sign problem, we can calculate thermodynamic quantities of 1D frustrated quantum systems down to low temperatures with high accuracy. In fact, the method is successfully applied to some frustrated spin ladder systems.<sup>16,17,18,19</sup> Following the implementation procedure described in Ref. 18, we calculate the magnetization and the susceptibility with the maximum number of the retained bases  $m = 200$ . We have confirmed that the computed data converge with respect to  $m$  and the Trotter number.

## III. DM RG RESULTS

In this section, we would like to describe the theoretical aspects of the zigzag chain on the basis of the DM RG calculations. In Fig. 3, we show the normalized susceptibilities  $\chi = J_1 / N (g_B)^2$  for  $J_1 > J_2$  and  $J_2 / N (g_B)^2$  for  $J_1 < J_2$ , where  $\chi$  is the magnetic susceptibility and  $N$  is the number of sites. For both cases, we can see that  $\chi$  exhibits the Curie-Weiss type behavior in a high temperature region. As temperature is decreased,  $\chi$  starts to decrease after taking a round peak, and finally converges to a finite value as  $T \rightarrow 0$  except for the Majumdar-Ghosh point ( $J_2 = J_1 = 0.5$ ),<sup>1</sup> where  $\chi$  rapidly decreases in the low temperature region.

For  $J_2 = J_1 < 0.2411$ , the zigzag chain has the gapless excitation and even in the dimer phase the spin gap is very small for  $J_2 = J_1 < 0.3$ .<sup>7,8</sup> Also for the nearly two chain case, the spin gap is exponentially small:  $\exp(-\text{const} / |J_2 - J_1|)$ .<sup>9</sup> The figures are clearly reflecting such gapless or nearly gapless behavior of the zigzag chain. Particularly for the case of  $J_1 < J_2$ , it can be seen that the temperature dependence of  $\chi$  is rather weak, implying that the dimer gap is very small in a wide range of  $0 < J_1 = J_2 < 0.5$ , which are consistent with the bosonization and the zero temperature DM RG predictions.<sup>9</sup> However, a notable point is that, for  $J_1 > J_2$ , the peak position shifts to the low temperature side as  $J_2 = J_1$  is increased, while for  $J_1 < J_2$ , the peak position stays at almost the same temperature. This fact is reflecting that the dimer gap grows rapidly near the Majumdar-Ghosh point,<sup>1</sup> whereas the chain of  $J_1 = J_2 = 0.5$  is still far away from the complete-dimer ground state.

We next discuss the magnetization curves, which are shown in Fig. 4. Both for  $J_1 < J_2$  and  $J_1 > J_2$ , we can see the characteristic property in the gapless Heisenberg chain as well. After the linear behavior with  $H$  is observed near the zero magnetic field ( $H = 0$ ), the magnetization  $M$  increases along a convex-down curve in the middle field region, and finally saturates near  $g_B H = J_1 (J_2) / 2.5$ . However, what we want to emphasize here is that the curve is quantitatively different from that of the pure Heisenberg chain. In particular, for

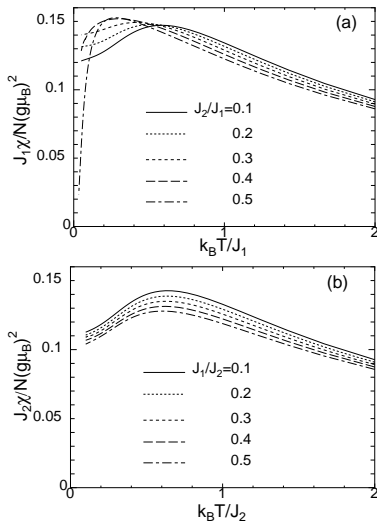


FIG. 3: Finite temperature DMRG results of the susceptibility (a) for  $J_1 > J_2$  and (b) for  $J_1 < J_2$ .

$J_1 > J_2$  the curves of various  $J_2=J_1$  seem to cross each other in the middle-eld region ( $g_B H = J_1 \cdot 1.3$ ), while for  $J_1 < J_2$ , they are uniformly shifting to the right-hand side as  $J_1=J_2$  is increased. These behaviors imply that the next-nearest interaction effect on the magnetization curve can appear rather clearly in the middle or high-eld region than in the low-eld region, which will play an important role in analyzing the magnetization curve of  $(N_2H_5)CuCl_3$ .

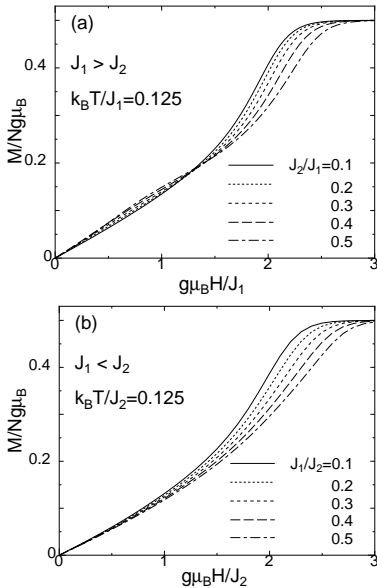


FIG. 4: The magnetization curves obtained with the DMRG (a) for  $J_1 > J_2$  at  $k_B T = J_1 \cdot 0.125$  and (b) for  $J_1 < J_2$  at  $k_B T = J_2 \cdot 0.125$ .

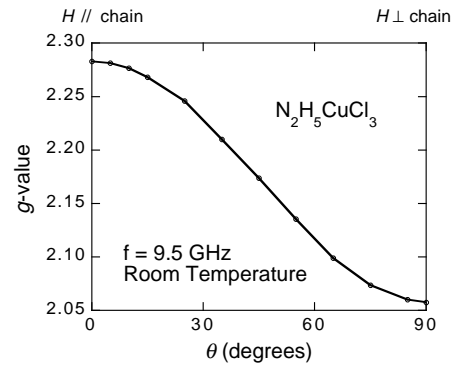


FIG. 5: The angular dependence of the  $g$ -value of  $(N_2H_5)CuCl_3$ .

#### IV. EXPERIMENTAL RESULTS

##### A. ESR and specific heat

We performed X-band ESR measurements at room temperature on a single crystal sample of  $(N_2H_5)CuCl_3$  in order to get the  $g$ -values precisely. A accurate comparison between the experimental data and the numerically calculated ones requires the precise  $g$ -values. Figure 5 shows the angular dependence of the  $g$ -value. We obtained the  $g$ -values of 2.285 and 2.060 for the external magnetic field parallel and perpendicular to the chain, respectively. In the following comparisons between experiments and calculations, we used these  $g$ -values.

We carried out specific heat measurements on a powder sample of  $(N_2H_5)CuCl_3$ . Figure 6 shows the temperature dependence of the specific heat divided by temperature. Here, the data include the lattice contribution. We observed an anomaly at 1.55 K ( $T_N$ ) which is probably due to the antiferromagnetic long-range ordering. In order to avoid three dimensional effect in this quasi-one-dimensional system, we carried out high-eld magnetization experiments at 2 K above  $T_N$ .

##### B. magnetic susceptibility

Magnetic susceptibility  $\chi_{EXP}$  of the single crystal of  $(N_2H_5)CuCl_3$  parallel to the chain, which was used for the ESR measurement, is presented in Fig. 7, where the DMRG results  $\chi_{DMRG}$  are also shown for comparison. In the high temperature region the  $\chi_{EXP}$  exhibits the Curie-Weiss-type  $T$ -dependence, and has a round peak around  $T = 10K$ . When the temperature is decreased further, the  $\chi_{EXP}$  also decreases and finally converges to a finite value in the zero temperature limit. Since these features are characteristic in gapless 1D antiferromagnets, we should take account of the two possibilities of the gapless zigzag chains, as mentioned in the introduction. We thus analyze  $\chi_{EXP}$  with the DMRG results both for the single chain limit ( $J_1 > J_2$ ) and the weakly coupled

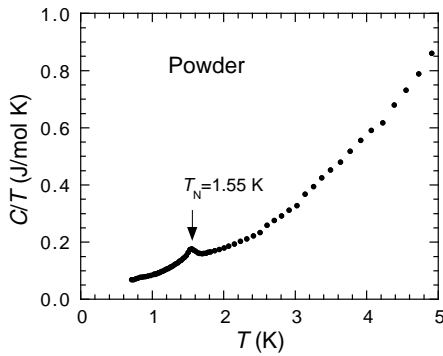


FIG. 6: The specific heat of a powder sample of  $(\text{N}_2\text{H}_5)\text{CuCl}_3$ .

Heisenberg chain limit ( $J_1 < J_2$ ). In fitting, we first estimate the dominant exchange coupling constant from the position of the broad peak, by using  $g = 2.285$  obtained from the ESR, and then tune another exchange coupling constant so as to reproduce the shape of the susceptibility well.

For the former case ( $J_1 > J_2$ ), we find that  $\chi_{\text{DMRG}}$  of  $J_2 = J_1 = 0.1$  with  $J_1/k_B = 17.4$  K agrees well with  $\chi_{\text{EXP}}$  in the whole temperature region (see Fig. 7 (a)). For the latter case ( $J_1 < J_2$ ), we can also see that the DMRG results for  $0.2 < J_1 = J_2 < 0.3$  well reproduce the shape of the experimental susceptibility as in Fig. 7 (b), where the best fitted value is obtained as  $J_1 = J_2 = 0.25$  with  $J_2/k_B = 16.3$  K. Since the DMRG results seem to explain the whole shape of the susceptibility well for both cases, we can unfortunately find no decisive information in the susceptibility to confirm which case is realized in  $(\text{N}_2\text{H}_5)\text{CuCl}_3$ . Here it should be noted that, also for the case of H $\perp$  chain, very similar results were obtained using the same parameter values of the exchange couplings as for H// chain and  $g = 2.060$  obtained from ESR. Therefore we next discuss the consistency with the magnetization curve.

Before proceeding to the next subsection we make a comment about a possibility of the weak ferromagnetic coupling. We have also computed the case of a negative  $J_2$  ( $J_1$ ) for  $J_1 > J_2$  ( $J_1 < J_2$ ). However, the shape of the susceptibility is changed drastically by introducing the ferromagnetic coupling, and so that the couplings of  $(\text{N}_2\text{H}_5)\text{CuCl}_3$  are antiferromagnetic.

### C. Magnetization curve

Figure 8 shows the magnetization curve for the single crystal of  $(\text{N}_2\text{H}_5)\text{CuCl}_3$  along the chain at  $T = 2.0$  K up to 30 T. The temperature was set a little above  $T_N$  (1.55 K) as already mentioned. Around the saturation field, there is a small hysteresis of magnetization between the ascending and descending processes, due to the magneto-caloric effect. In the figure, we can see that the measured curve of  $(\text{N}_2\text{H}_5)\text{CuCl}_3$  is qualitatively similar to the gapless chain, which is consistent with the susceptibility results. Using the parameters estimated in the previous

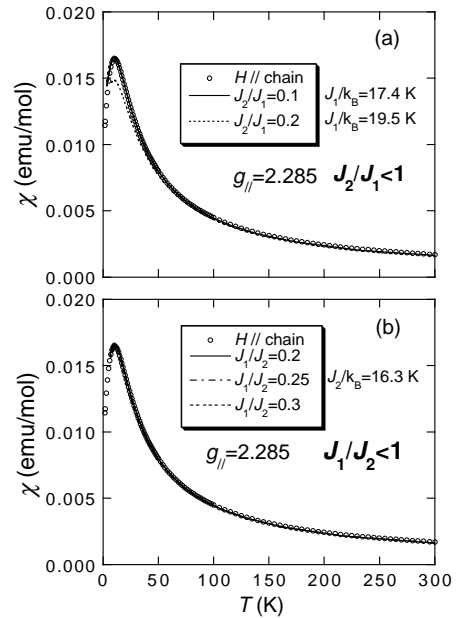


FIG. 7: Magnetic susceptibility of  $(\text{N}_2\text{H}_5)\text{CuCl}_3$ . The open circles denote experimental data  $\chi_{\text{EXP}}$  and the lines show finite temperature DMRG results  $\chi_{\text{DMRG}}$ .

subsection, we now discuss the magnetization processes of the DMRG and the experiments. The temperature used in the numerical calculations was determined close to that in the experiments.

The results of comparisons are also shown in Fig. 8, where the DMRG curves both for  $J_1 > J_2$  and for  $J_1 < J_2$  are in good agreement with the experimental one in the low-field region. However, the magnetization curve in the middle field and the high field regions is reproduced well by the coupling of  $J_1 = J_2 = 0.25$ , as can be seen in Fig. 8 (b). In fact, the calculated curve for  $J_1 > J_2$  is slightly winding around  $15 < H < 20$  T, while that for  $J_1 < J_2$  is well fitted in the all range of the magnetic field. As described in Sec. III, the effect of the frustration appears rather in middle and high-field region than in the low-field one. Hence we conclude that the zigzag chain compound  $(\text{N}_2\text{H}_5)\text{CuCl}_3$  has  $J_1 = J_2 = 0.25$  with  $J_2 = 16.3$  K.

### V. SUMMARY AND DISCUSSION

We have investigated magnetic properties of  $(\text{N}_2\text{H}_5)\text{CuCl}_3$ , which can be regarded as a zigzag chain with the coupling  $J_1 < J_2$  by the accurate comparison between the numerical calculations and experiments.

First, we have calculated the susceptibility and the magnetization curve of the zigzag chain using the finite temperature DMRG method; the obtained results for  $J_1 > J_2$  ( $J_1 < J_2$ ) show gapless or nearly gapless behavior of the susceptibility and the magnetization curve

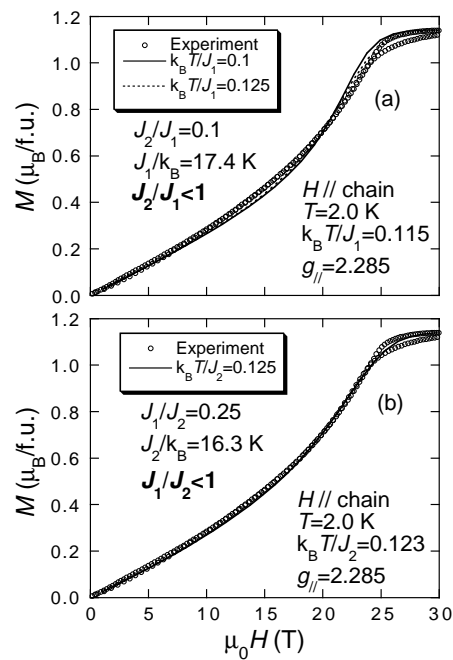


FIG. 8: The magnetization curves of  $(\text{N}_2\text{H}_5)\text{CuCl}_3$ . The comparison with the DMRG results (a) for  $J_2=J_1 = 0.1$  and (b) for  $J_1=J_2 = 0.25$ .

in  $0 < J_2=J_1 < 0.4$  ( $0 < J_1=J_2 < 0.5$ ), which supports the fact that the spin gap is fairly small. Although the magnetization curves for  $J_1 > J_2$  and  $J_1 < J_2$  show the similar gapless behavior in the low field region, the quantitative difference appears rather in the middle and high field region.

We have next presented the experimental results for the single crystal of  $(\text{N}_2\text{H}_5)\text{CuCl}_3$ . The  $g$ -values parallel and perpendicular to the chain are determined as  $g = 2.285$  and  $2.060$ , respectively by the ESR experiment. The Néel temperature is also estimated as  $T_N = 1.55\text{K}$  from the specific heat of a powder sample. Above the Néel temperature, the observed susceptibility and the magnetization for the single crystal show gapless or nearly gapless behavior. By comparing the experimental data with the DMRG results, we have determined the exchange coupling  $J_1=J_2 = 0.25$  with  $J_2=k_B = 16.3\text{K}$ . Therefore we have concluded that  $(\text{N}_2\text{H}_5)\text{CuCl}_3$  can be viewed as weakly coupled Heisenberg chains with a frustrated interaction.

In the present paper, we have addressed the zigzag compound of  $(\text{N}_2\text{H}_5)\text{CuCl}_3$  in terms of the bulk quantities: the magnetic susceptibility and the high field magnetization, for which the rather precise analyses are required. However, the frustration effect often gives rise to the incommensurate behavior in the correlation function,<sup>9,20</sup> which is difficult to be captured with the bulk quantities. Thus it is also an interesting problem to investigate the compound by measurements of the fluctuation-associated quantities with the position resolvable methods, such as NMR or the inelastic neutron scattering.

Acknowledgments

This work was partly supported by the Grand-in-Aid for Scientific Research from the Japanese Ministry of Education, Culture, Sports, Science and Technology. The experimental work was carried out under visiting Researcher's Program of KYOKUGEN, Osaka University.

<sup>1</sup> C. K. Majumdar and D. K. Ghosh, *J. Math. Phys.* **10**, 1388 (1969).  
<sup>2</sup> F. D. M. Haldane, *Phys. Rev. B* **25**, 4925 (1982).  
<sup>3</sup> T. Hamada, J. Kane, S. Nakagawa, and Y. Natsume, *J. Phys. Soc. Jpn.* **57**, 1891 (1988).  
<sup>4</sup> M. P. Gelfand, *Phys. Rev. B* **43**, 8644 (1991).  
<sup>5</sup> C. Lhuillier and G. Misguich, cond-mat/0109146, and references therein.  
<sup>6</sup> J. des Cloizeaux and J. J. Pearson, *Phys. Rev.* **128**, 2131 (1962).  
<sup>7</sup> T. Tonegawa and I. Harada, *J. Phys. Soc. Jpn.* **56**, 2153 (1987).  
<sup>8</sup> K. Okamoto and K. Nomura, *Phys. Lett. A* **169**, 433 (1992).  
<sup>9</sup> S. R. White and I. A. Aeschlimann, *Phys. Rev. B* **54**, 9862 (1996).  
<sup>10</sup> M. Matsuda and K. Katsumata, *J. Mag. Mag. Mat.* **140-144**, 1671 (1995).  
<sup>11</sup> H. Kikuchi, H. Nagasawa, Y. Ajiro, T. Asano, and T. Goto, *Physica B* **284-288**, 1631 (2000).

<sup>12</sup> D. B. Brown, J. A. Donner, J. W. Hall, S. R. Wilson, R. B. Wilson, D. J. Hodgson, and W. E. Hatfield, *Inorg. Chem.* **18**, 2635 (1979).  
<sup>13</sup> M. Hagiwara, Y. Nambu, K. Kindo, N. Maeshima, K. Okunishi, T. Sakai, M. Takahashi, *Physica B* **294-295**, 83 (2001).  
<sup>14</sup> X. Wang and T. Xiang, *Phys. Rev. B* **56**, 5061 (1997).  
<sup>15</sup> N. Shibata, *J. Phys. Soc. Jpn.* **66**, 2221 (1997).  
<sup>16</sup> K. M. Aisinger and U. Schollwöck, *Phys. Rev. Lett.* **81**, 445 (1998).  
<sup>17</sup> A. Klumper and R. Ruppach and F. Schönlank, *Phys. Rev. B* **59**, 3612 (1999).  
<sup>18</sup> N. Maeshima and K. Okunishi, *Phys. Rev. B* **62**, 934 (2000).  
<sup>19</sup> Ch. Waldmann, H. Kreutzmann, U. Schollwöck, K. M. Aisinger, and H.-U. Everts, *Phys. Rev. B* **62**, 9472 (2000).  
<sup>20</sup> S. Watanabe and H. Yokoyama, *J. Phys. Soc. Jpn.* **68**, 2073 (1999).